nature ecology & evolution

Supplementary information https://doi.org/10.1038/s41559-024-02570-x

Anthropogenic land consolidation intensifies zoonotic host diversity loss and disease transmission in human habitats

In the format provided by the authors and unedited

Contents of this file

Overview of study system

Supplementary Figures 1-16

Supplementary Tables 1- 4

Overview of study system

Our research site is located Hu region (108.6° E, 34.1° N) in Shanxi Province, Central China. Nine trapping sites were established on agricultural land near residential areas (Box 1). More than 15,000 rodents of 9 species were trapped, comprising >300,000 trap-nights in total from 1980-2022. The trapped species include the striped field mouse, Norway rat, buff-breasted rat, rat-like hamster, house mouse, black rat, Chinese white-bellied rat, harvest mouse and unknown species. The striped field mouse is targeted by anti-rodent Campaigns in Hu region. In this study, we primarily focus on three most abundant species: the striped field mice, Norway rats, and buff-breasted rat together account for 88% of the total rodent number.

The striped field mouse exhibits a high level of food plasticity and behavioral flexibility, making it an adaptable omnivorous species [1,2]. Found in various habitats such as agricultural lands, urban areas, and forest edges, striped field mice are proficient at spatial exploration and display boldness in their behavior [1]. Their dispersal across different biotopes, coupled with rapid population growth, imposes competitive pressure on other small mammal species [3,4]. Norway rats are well-known for their close association with human populations and their widespread distribution across diverse urban and rural environments [5,6]. Their dietary habits are remarkably flexible, as they consume a wide array of foods, including cereal grains, fish, meats, nuts, and fruits [5]. While their dispersal is generally limited to short distances, they are capable of occasional long-distance movements [7,8]. Similarly, the buff-breasted rat also exhibits omnivorous feeding habits, with a preference for plant-based foods such as seeds, nuts, acorns and crop seeds [9]. Inhabiting a variety of environments including farmlands, forests and urban areas, buff-breasted rats are adept at colonizing new areas and have the ability to disperse over long distances. Overall, these three numerically dominant rodent species exhibit significant overlap in their habitats and dietary preferences, leading to interspecific competition.

Importantly, among those synanthropic rodents, the striped field mouse is the main reservoir host of Hantaan virus (HTNV), a negative-sense single-stranded RNA virus capable of causing a zoonotic disease hemorrhagic fever with renal syndrome (HFRS) in humans. HNTV is primarily transmitted to humans through inhalation of aerosolized viral particles shed in rodent urine, saliva, and feces [10,11]. Moreover, HTNV transmission dynamics are influenced by temperature, rainfall, host population density, and land-use. Specifically, increased rainfall and comfortable temperature can lead to abundant food resources and suitable breeding grounds for rodents, resulting in population booms. Consequently, higher host densities may amplify HTNV transmission through increasing opportunities for virus spillover to humans. Furthermore, anthropogenic landscape change can alter the dynamics of hantaviruses transmission [12,13].

Supplementary Figures

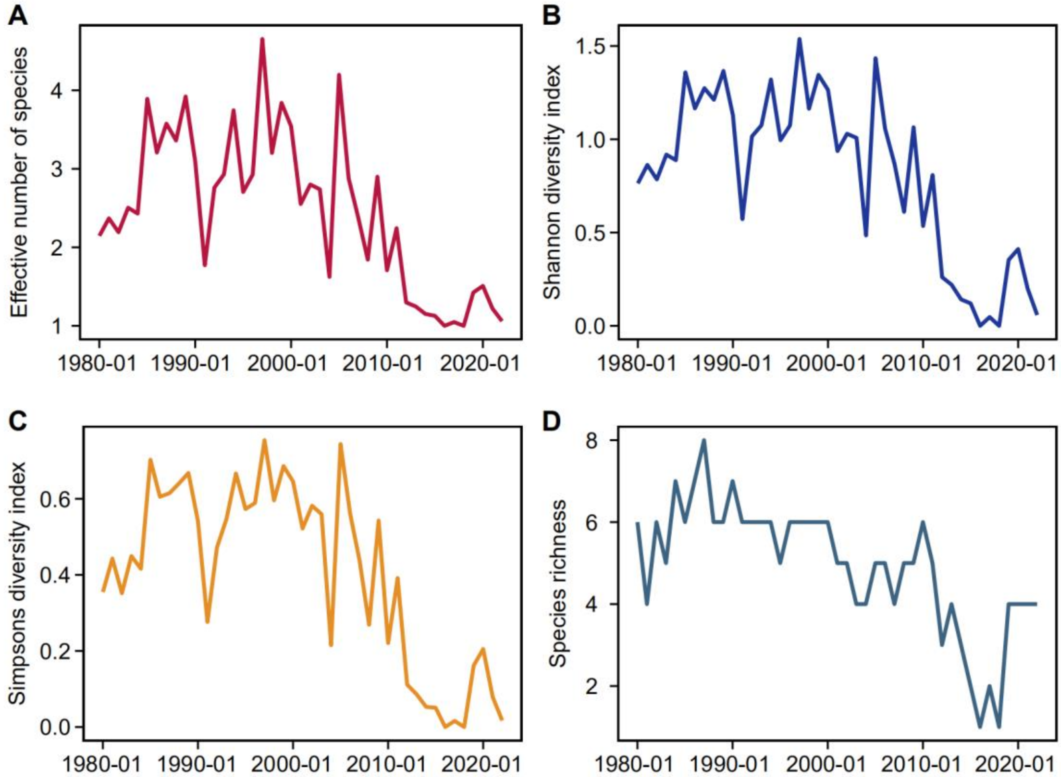

Supplementary Fig. 1: Rodent diversity measured by **(A)** the effective number of species, **(B)** Simpson’s diversity index, **(C)** Shannon-Wiener diversity index, and **(D)** species richness, from 1980-2022. Species richness is defined as the number of species identified in a given year. Higher values for the Shannon-Weiner, Simpson's diversity index, and effective number of species indicate greater biodiversity. As the Shannon-Wiener and Simpson's diversity index are strongly correlated ($\rho = 0.99$, $P < 0.001$), and the effective number is a more suitable alternative, we present only the effective number and species richness in the main text.

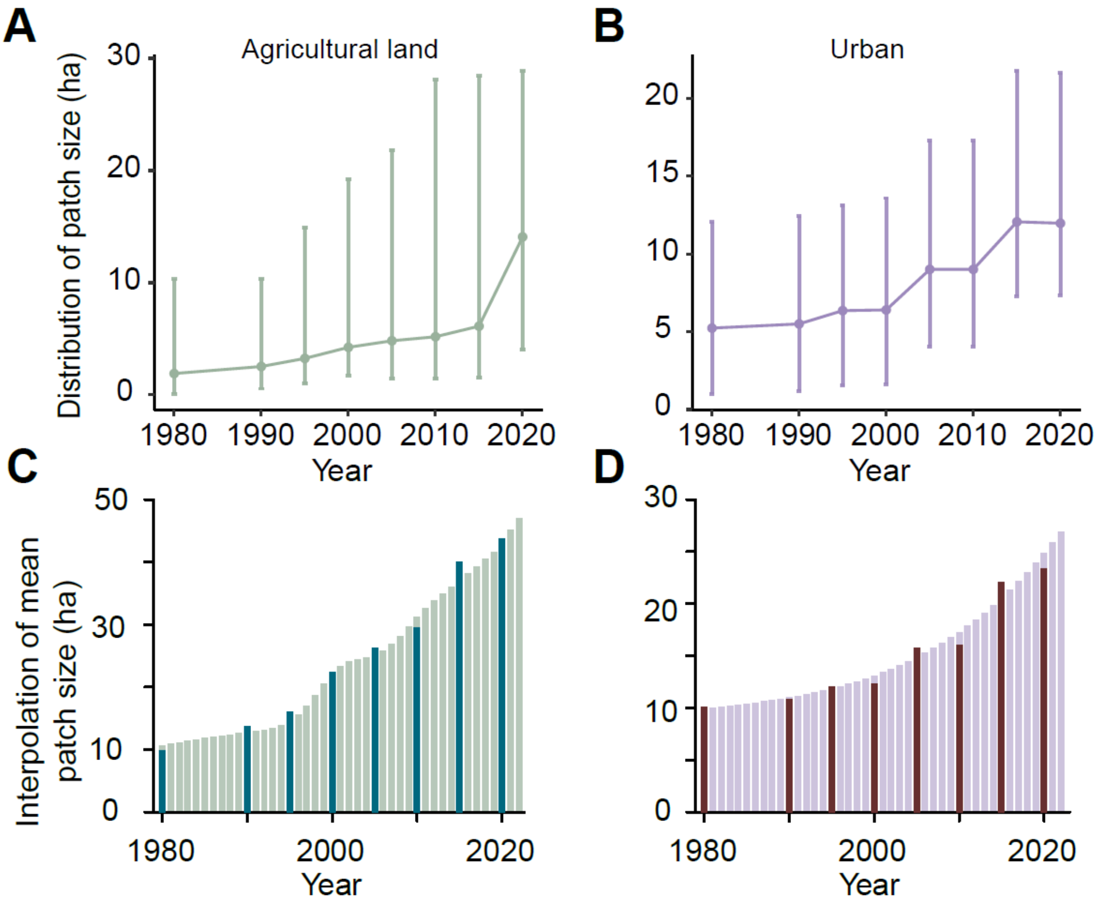

Supplementary Fig. 2: Distribution of patch size and interpolation of mean patch size. **(A)** Patch size range of agricultural land and **(B)** urban areas from 1980 - 2020. The dots show the medians, and the whiskers show the first (upper) and third quartiles (lower) of the patch sizes. **(C)** Mean patch sizes of agricultural land and **(D)** urban area from 1980-2022. A generalized additive model was used to interpolate the missing values. Dark colors represent the observed values (dark green and dark purple) and light colors represent the interpolated values.

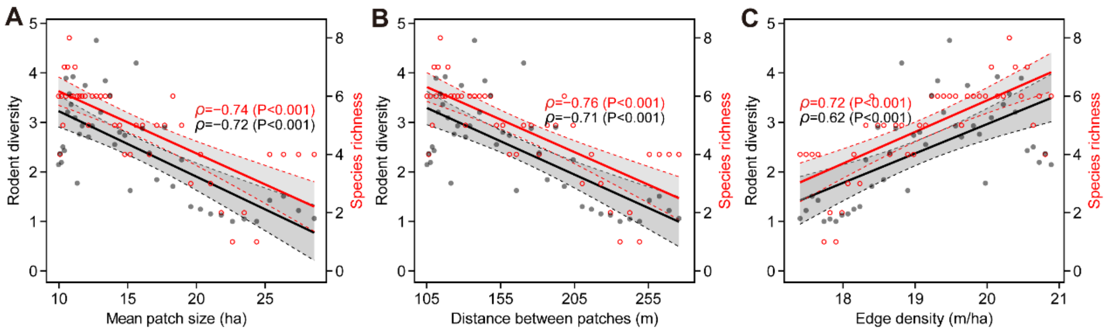

Supplementary Fig. 3: Association between rodent species diversity and land consolidation. **(A)** Rodent species diversity decreased with mean patch size. **(B)** Rodent species diversity decreased with the distance between patches. **(C)** Rodent species diversity increased with edge density. The scatterplot shows the association between land consolidation and rodent species diversity (left y-axis, black dots, effective number of species) and species richness (right y-axis, red circles, species richness), assessed with Spearman's rank correlation coefficient (ρ). Lines represent fitted linear regression models (shading shows 95% confidence intervals of fitted values).

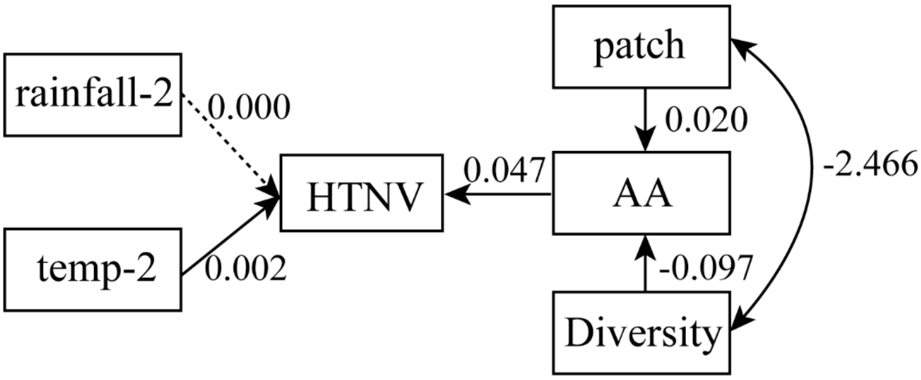

Supplementary Fig. 4: Schematic, including results, of our structural equation models for HTNV transmission dynamics (χ^2/df = 10.04/8, comparative fit index = 0.99). Double-headed arrows indicate correlations. Straight lines indicate direct relationships. The values associated with the arrows are standardized path coefficients. The dashed lines represent nonsignificant paths; '-2', lag by two months; rainfall, monthly average rainfall; 'temp', monthly average temperature; patch, mean patch size; HTNV, carrying rate of HTNV in the striped field mouse; AA, the percentage of striped field mice among all rodents; Diversity, rodent species diversity in the Hu region.

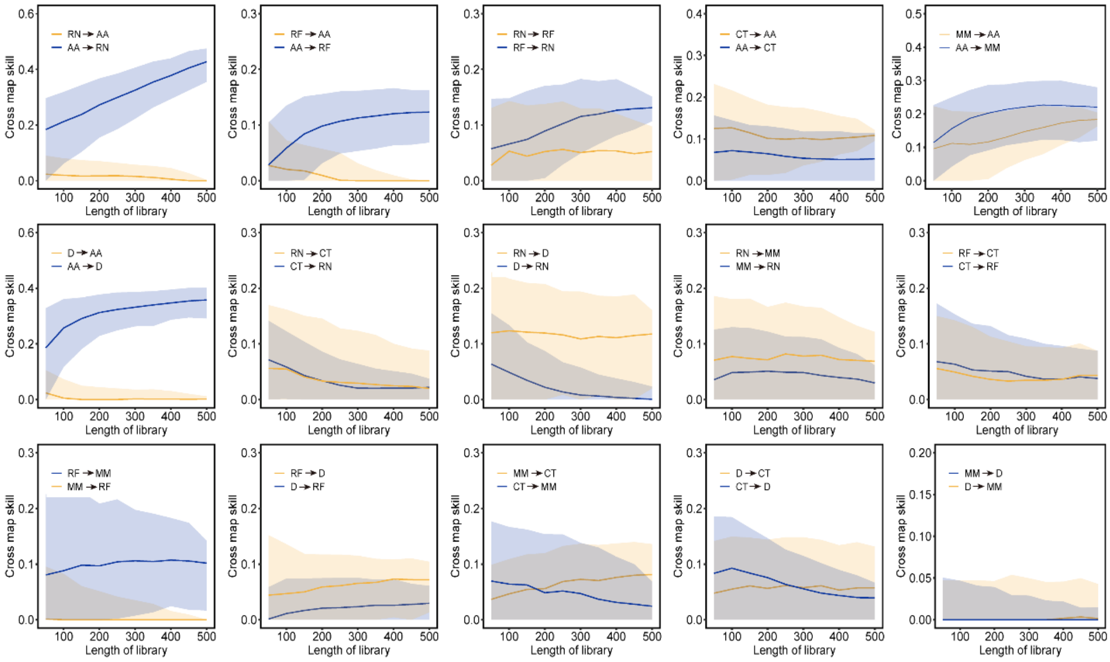

Supplementary Fig. 5: Convergent cross-map (CCM) detect interspecific causality for rodent population dynamics. Interactions between striped field mouse (*AA*), Norway rat (*RN*), buff-breasted rat (*RF*), rat-like hamster (*CT*), house mouse (*MM*), black rat (*RR*), and an unknown species (*D*). The strength of the interaction between each pair of rodent species was assessed with the convergent cross-map skill, of which the value ranges from 0-1. Shaded regions represent the 95% credible intervals. *AA*→*RN*, i.e. the effect of species *AA* on species *RN*. Length of library refers to the number of data points used to construct the mapping.

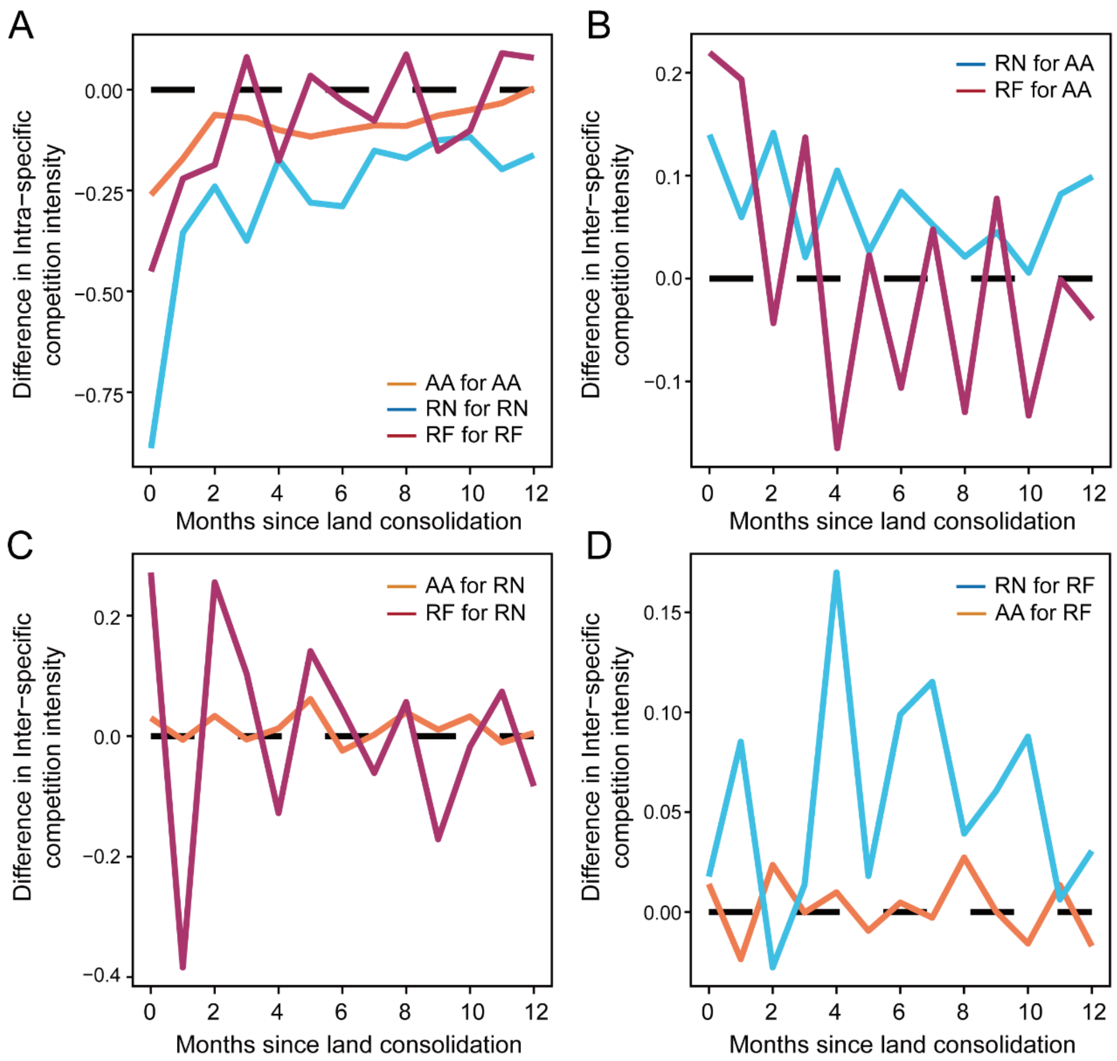

Supplementary Fig. 6: Difference in the intensity of species competition under the scenario land consolidation and the scenario without land change. (A) Difference in intraspecific competition intensity under the scenario land consolidation and the scenario without land change. The cumulative difference is negative. (B-D) Difference in interspecific competition intensity under the scenario land consolidation and the scenario without land change**.** The cumulative difference is positive. Compared to the scenario without land change, land consolidation suppresses the intraspecific competition and intensifies the interspecific competition among rodent species.

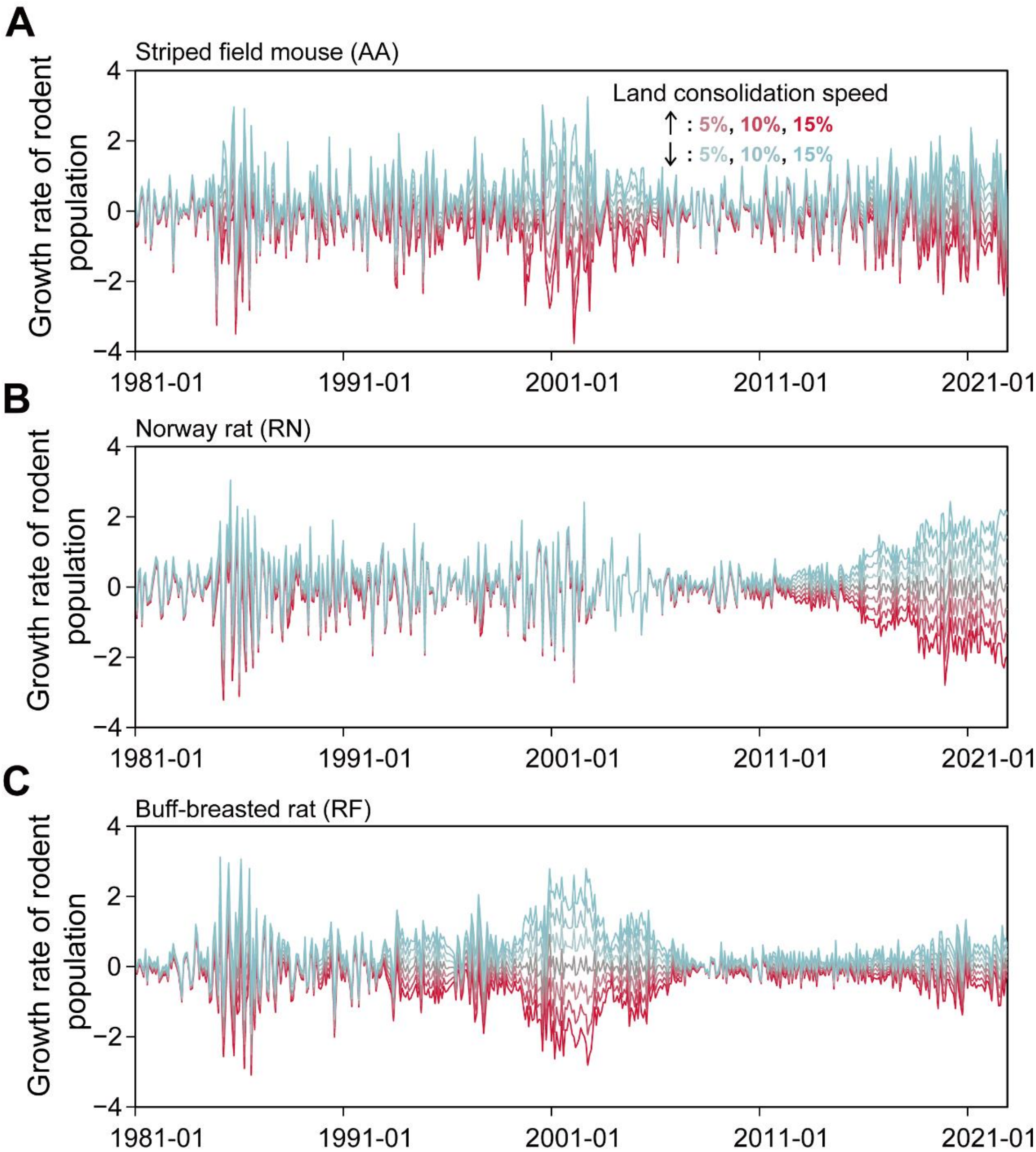

Supplementary Fig. 7: Land consolidation speed affects the rodent population growth rate. The plots show the response of the rodent population growth rate (A = striped field mouse, B =Norway rat, C = buff-breasted rat) to different speeds of land consolidation. Red: land consolidation speeds up by 5%, 10% and 15%; Blue: land consolidation slows down by 5%, 10% and 15%.

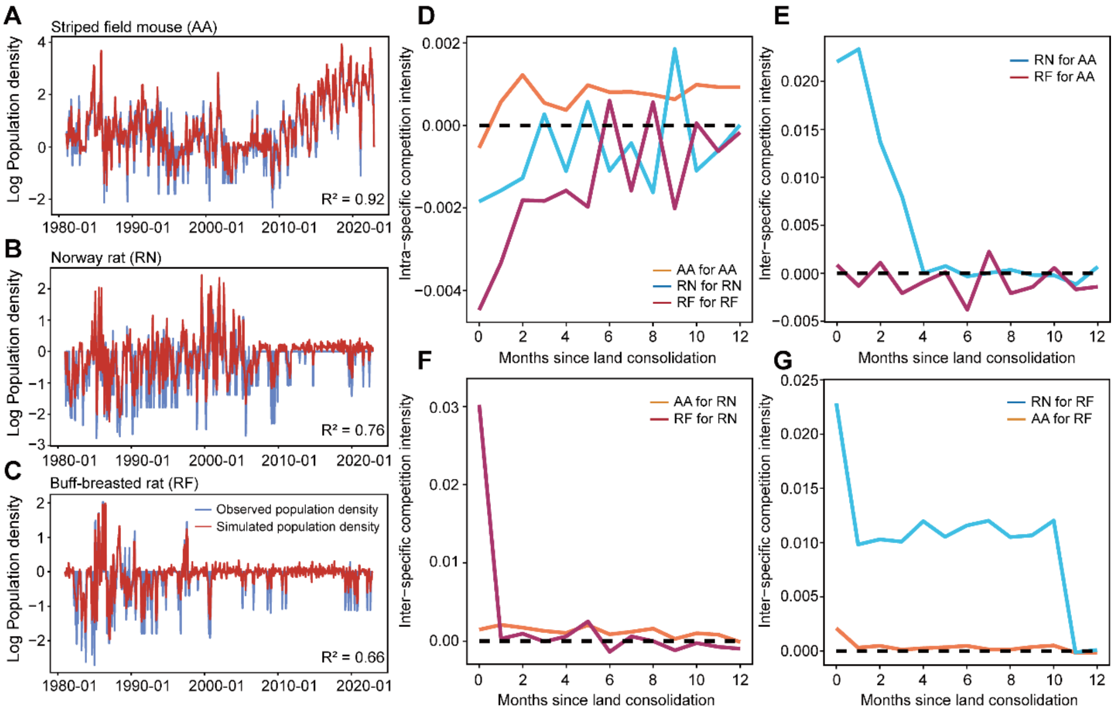

Supplementary Fig. 8: Sensitivity analysis for substituting mean patch size with agriculture patch area in the three-species dynamic model. **(A-C)** Estimated logarithm of the rodent population density (red lines) and the observed values (blue lines). Rodent population density for each species is expressed as capture numbers per 100 trap nights. **(D)** The effect of land consolidation on intraspecific competition. **(E-G)** The effect of land consolidation on interspecific competition.

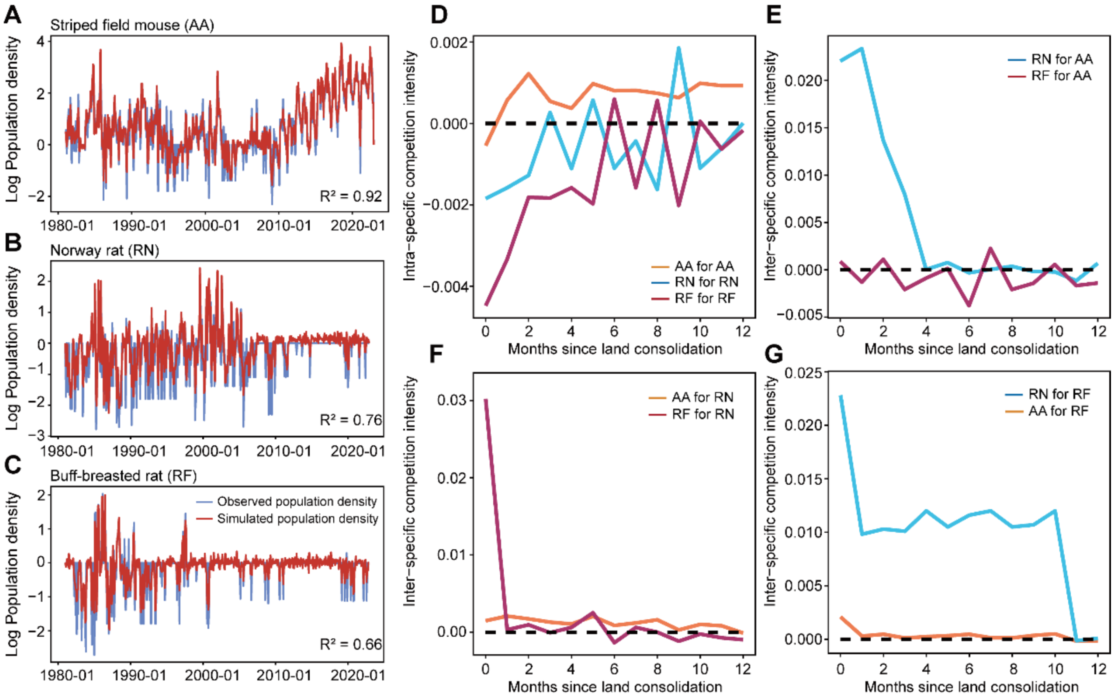

Supplementary Fig. 9: Sensitivity analysis for substituting mean patch size with urban patch area in the three-species dynamic model. **(A-C)** Estimated logarithm of the rodent population density (red lines) and the observed values (blue lines). Rodent population density for each species is expressed as capture numbers per 100 trap nights. **(D)** The effect of land consolidation on intraspecific competition. **(E-G)** The effect of land consolidation on interspecific competition.

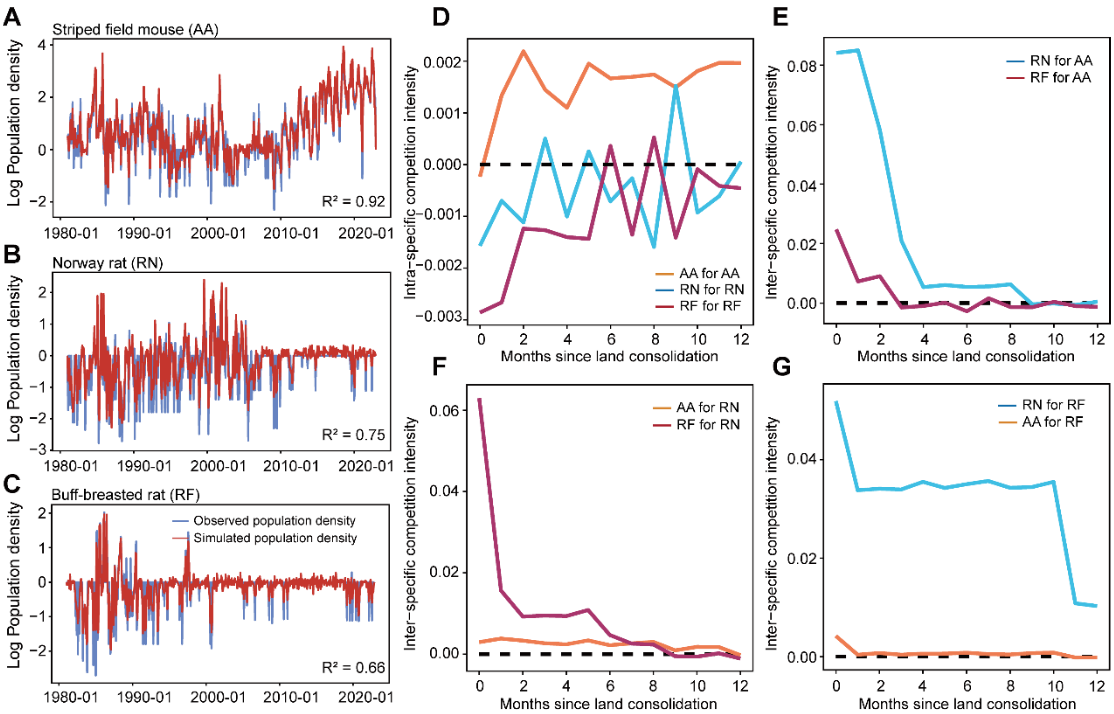

Supplementary Fig. 10: Sensitivity analysis for substituting mean temperature with daily maximum temperature in the three-species dynamic model. **(A-C)** Estimated logarithm of the rodent population density (red lines) and the observed values (blue lines). Rodent population density for each species is expressed as capture numbers per 100 trap nights. **(D)** The effect of land consolidation on intraspecific competition. **(E-G)** The effect of land consolidation on interspecific competition.

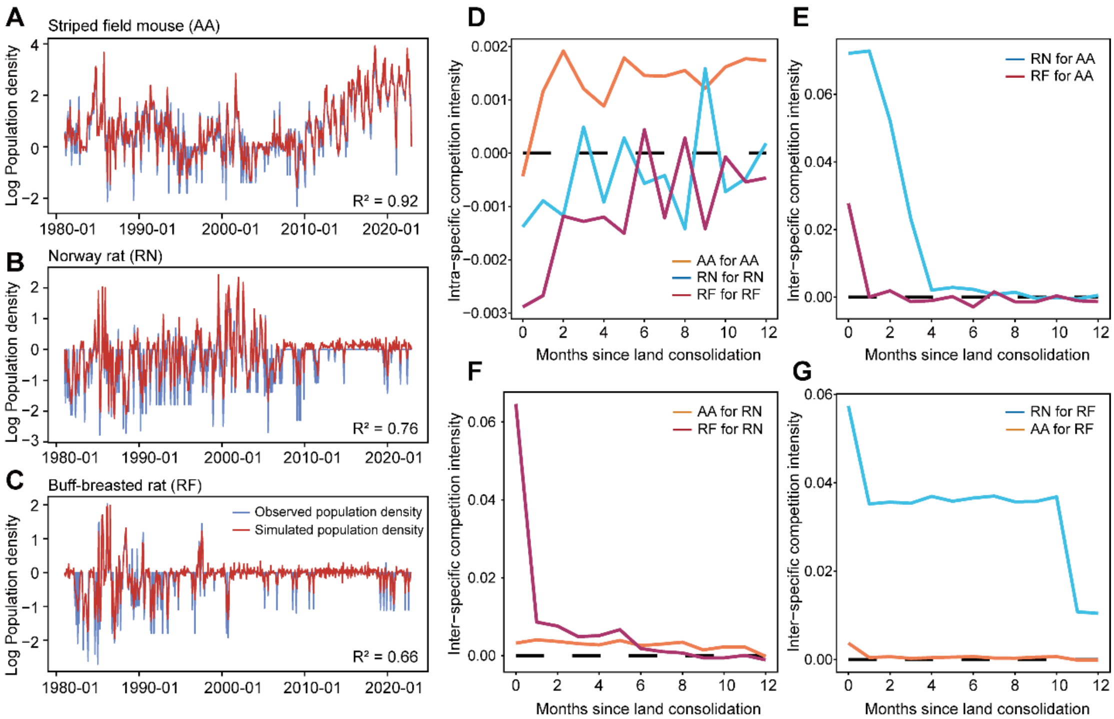

Supplementary Fig. 11: Sensitivity analysis for land consolidation speed accelerated by 10% in the three-species dynamic model. **(A-C)** Estimated logarithm of the rodent population density (red lines) and the observed values (blue lines). Rodent population density for each species is expressed as capture numbers per 100 trap nights. **(D)** The effect of land consolidation on intraspecific competition. **(E-G)** The effect of land consolidation on interspecific competition.

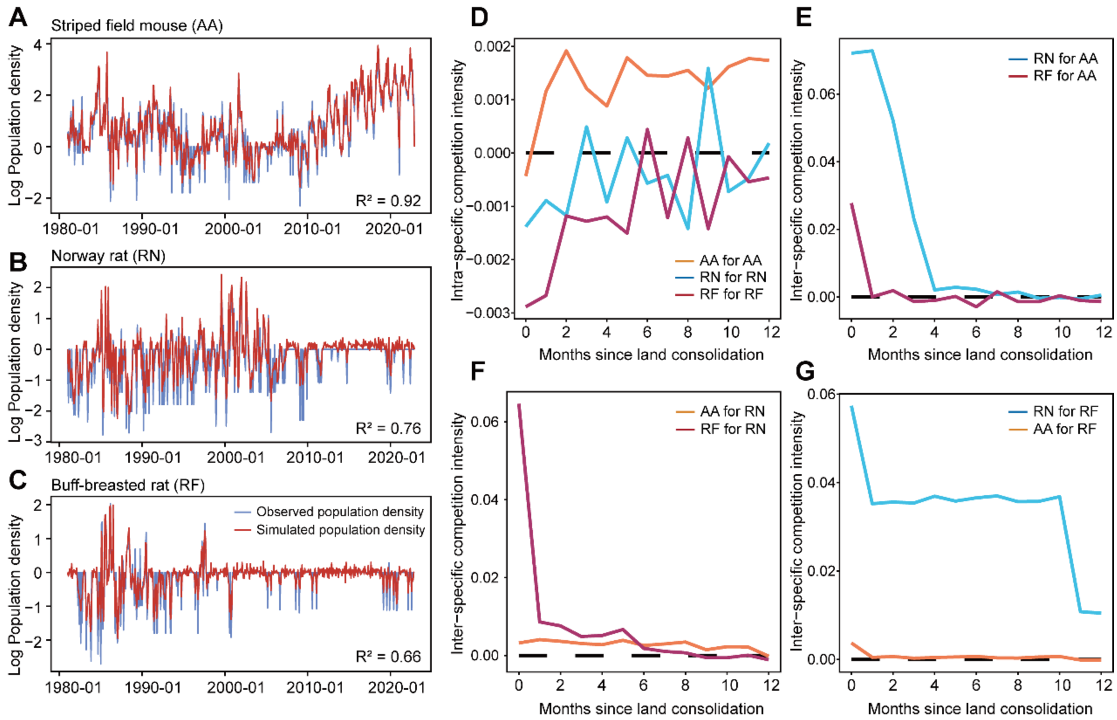

Supplementary Fig. 12: Sensitivity analysis for land consolidation speed deceleration by 10% in the three-species dynamic model. **(A-C)** Estimated logarithm of the rodent population density (red lines) and the observed values (blue lines). Rodent population density for each species is expressed as capture numbers per 100 trap nights. **(D)** The effect of land consolidation on intraspecific competition. **(E-G)** The effect of land consolidation on interspecific competition.

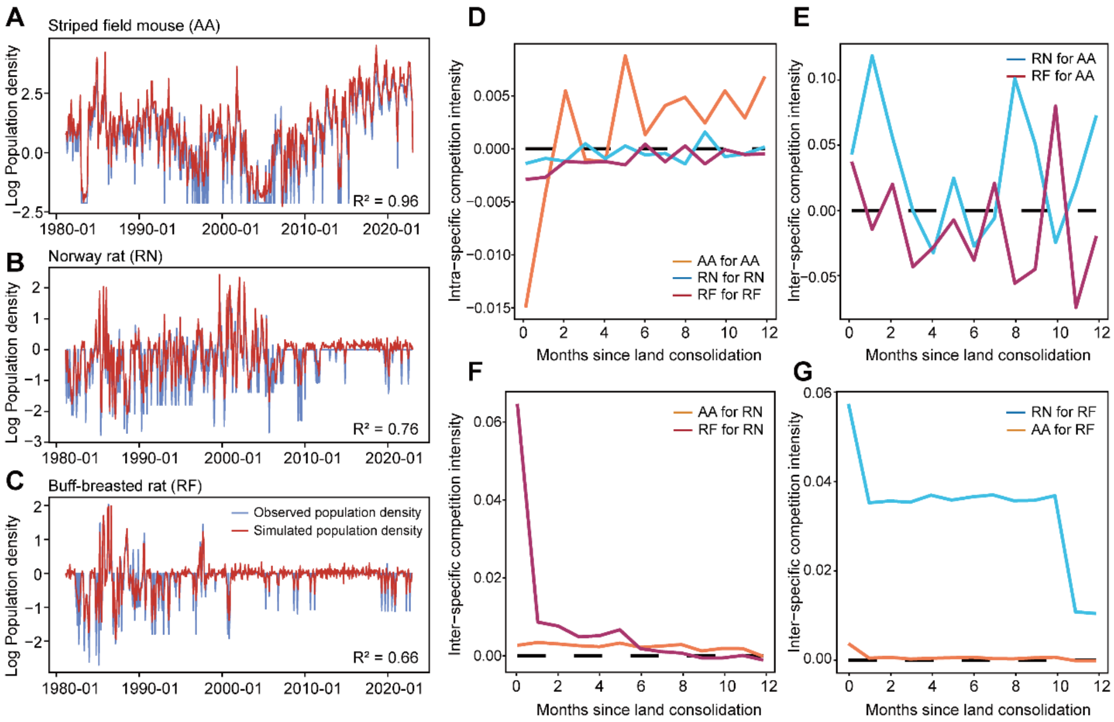

Supplementary Fig. 13: Sensitivity analysis for a 20% increase in the population density of striped field mice in the three-species dynamic model [14]. **(A-C)** Estimated logarithm of the rodent population density (red lines) and the observed values (blue lines). Rodent population density for each species is expressed as capture numbers per 100 trap nights. **(D)** The effect of land consolidation on intraspecific competition. **(E-G)** The effect of land consolidation on interspecific competition.

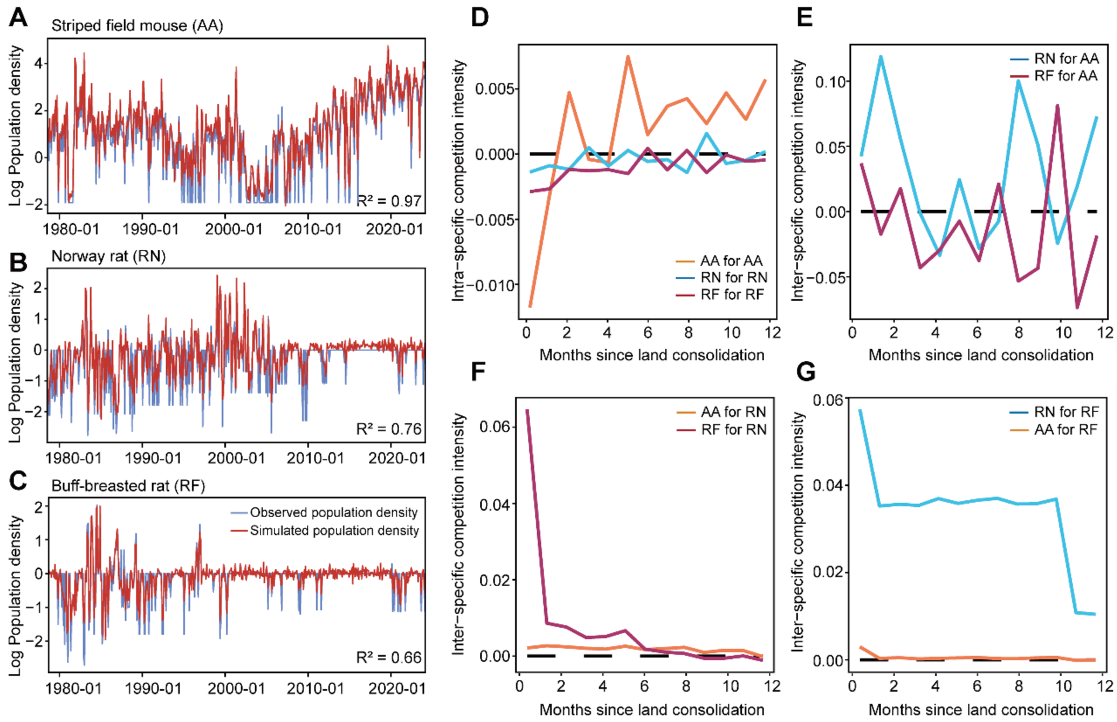

Supplementary Fig. 14: Sensitivity analysis for a 50% increase in the population density of striped field mice in the three-species dynamic model [14]. **(A-C)** Estimated logarithm of the rodent population density (red lines) and the observed values (blue lines). Rodent population density for each species is expressed as capture numbers per 100 trap nights. **(D)** The effect of land consolidation on intraspecific competition. **(E-G)** The effect of land consolidation on interspecific competition.

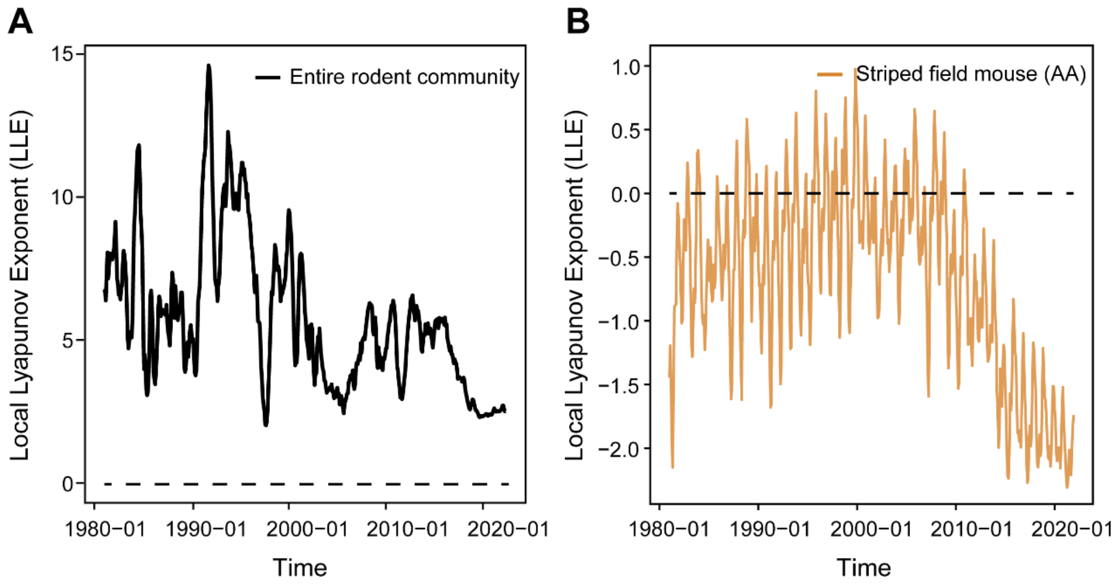

Supplementary Fig. 15: Time series of the local Lyapunov exponent (LLE). (A) The LLE for the entire rodent community comprising striped field mouse (*AA*), Norway rat (*RN*), and buff-breasted rat (*RF*) simultaneously. (B) The LLE specifically for striped field mouse. The LLE is calculated as the average rate of trajectory divergence (or convergence) over a time span of 6 mo. Lyapunov exponents were calculated from the Jacobian matrices of the nonlinear time series model (as in Eqn. 4).

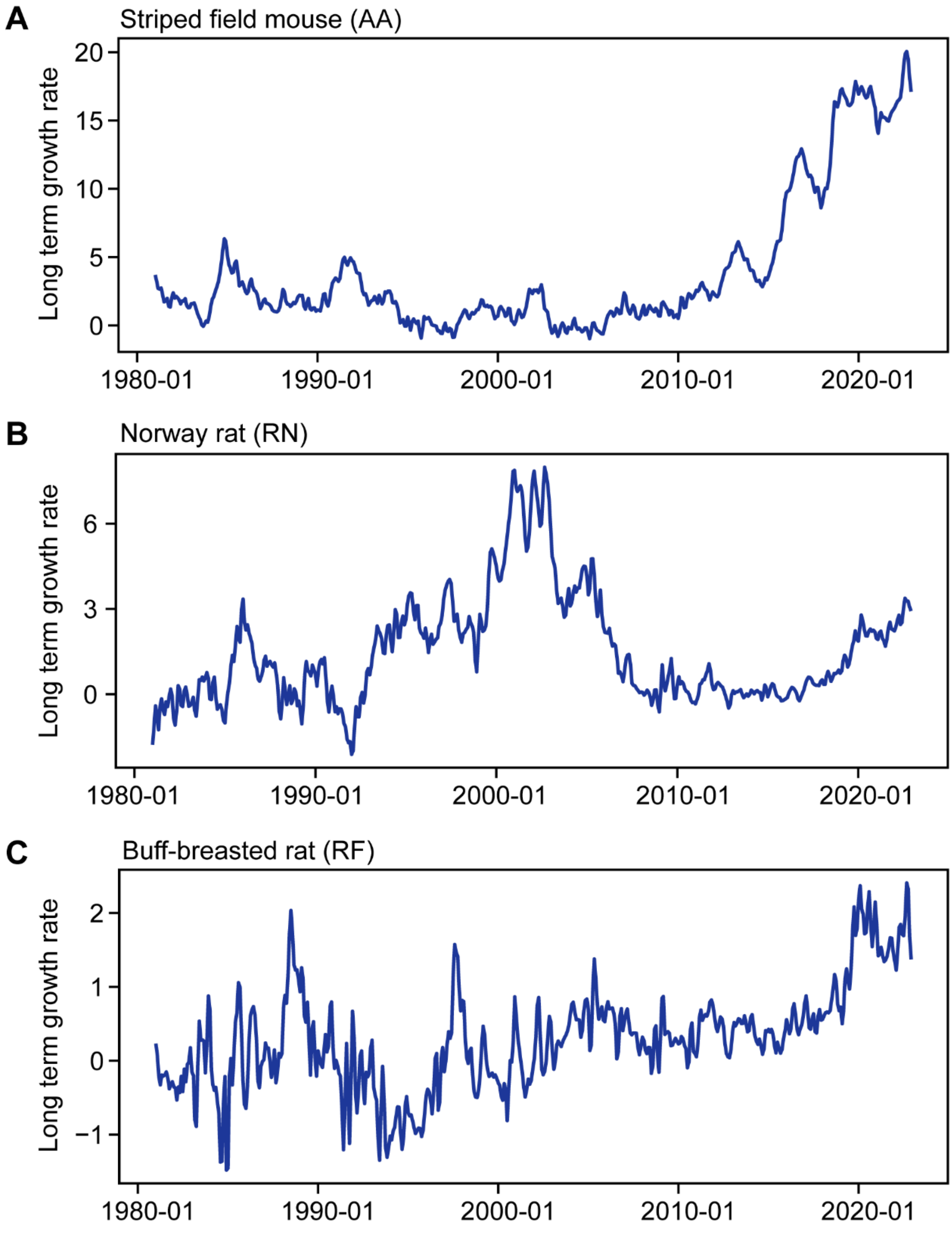

Supplementary Fig. 16: Parameters for long term growth rate of rodent population in three-species dynamic model. (A-C) Estimated values of long-term growth rate of rodent population (r_{lt}) for *AA*, *RN*, and *RF*.

Supplementary Table 1: Results of the multiple regression model diagnosis.

Variables	VIF	Tolerance	Condition Index
rainfall	1.567	0.638	1.000
temperature	1.635	0.611	3.329
AA density	2.331	0.429	6.242
mean patch size	247.008	0.004	3.385
distance between patches	404.387	0.002	123.127
edge density	42.949	0.023	480.260

VIF (variance inflation factor) greater than 10, tolerance less than 0.1, and condition index greater than 30 indicate significant multicollinearity.

Supplementary Table 2: *p*-value for rejecting the null hypothesis in random surrogate test.

	AA	***RN***	***RF***
AA	NA	0.678	0.734
RN	0	NA	0.02
RF	0.018	0.144	NA

Hopping to reject the null hypothesis that the obtained CCM results come from random noise rather than the internal patterns of time series, a null expectation was provided by running the causality test on the surrogate time series using the method of "seasonal". Each variable was tested separately with 500 random surrogates of the other two variables. In the case of *AA*→*RN*, it is significant in relation to a surrogate null distribution (p =0 <0.05), which indicates that *AA* leads to changes in *RN*. Regarding *RN*→*AA*, it is not quite significant at the 95th percentile of the null distribution. This may due to the complex and weak interactions between species that are difficult to detect. *AA*: Striped field mice, *RN*: Norway rats, and *CT*: rat-like hamsters.

Supplementary Table 3: Parameters in three-species population dynamics model.

striped field mouse (*AA*) population													
ε_{AA}	0.32	0.03	0.02	0.08	0.11	0.09	0.08	0.07	0.05	0.06	0.03	-0.01	-0.03
ε_{RN}	-0.51	-0.12	-0.29	0.21	-0.10	0.17	0.02	0.10	-0.17	0.15	-0.06	0.08	0.01
ε_{RF}	-1.26	-1.39	-0.89	-0.45	-0.07	-0.18	-0.12	-0.14	-0.14	0.02	-0.05	-0.00	-0.11
r_{rain}	0.00	0.07	-0.02	-0.02	0.02	0.01	0.00	0.00	0.00	0.00	0.00		
r_{temp}	-0.01	-0.25	0.06	0.05	-0.03	0.00	-0.01	-0.01	0.02	0.01	0.00		
Norway rat (RN) population													
ε_{AA}	-0.09	-0.06	-0.10	-0.05	-0.07	-0.11	-0.03	-0.06	-0.09	-0.04	-0.06	-0.02	0.00
ε_{RN}	-0.94	0.29	-0.33	-0.17	0.07	-0.20	-0.08	0.04	-0.08	0.16	0.01	-0.08	0.08
ε_{RF}	0.90	0.36	0.24	0.39	0.17	0.28	0.29	0.15	0.16	0.12	0.10	0.19	0.16
r_{rain}	0.01	0.03	-0.01	0.02	-0.01	0.00	0.00	0.00	0.00	0.00	0.00		
r_{temp}	-0.01	-0.10	-0.17	-0.15	-0.02	-0.02	0.01	-0.02	0.00	0.02	0.01		
buff-breasted rat (RF) population													
ε_{AA}	-0.10	0.02	-0.04	-0.01	-0.02	0.00	-0.01	0.00	-0.04	-0.01	0.01	-0.01	0.02
ε_{RN}	0.49	0.25	0.22	-0.03	0.20	-0.01	0.02	0.09	-0.10	0.15	0.11	-0.11	-0.08
ε_{RF}	-0.72	-0.54	-0.42	-0.47	-0.62	-0.47	-0.54	-0.57	-0.49	-0.51	-0.53	-0.14	-0.15
r_{rain}	0.00	0.05	-0.02	0.01	0.01	0.01	0.00	0.00	0.00	0.00	0.00		
r_{temp}	-0.04	-0.25	-0.18	-0.08	-0.04	-0.04	0.00	-0.01	0.02	-0.01	0.02		

Parameters ε_{AA}, ε_{RN}, and ε_{RF} are the intercept terms that quantify the effect of the patch size change on the resource occupation of species *AA*, *RN*, and *RF*, respectively. r_{rain} is the effect of rainfall on intrinsic growth rate. r_{temp} is the effect of temperature on intrinsic growth rate.

Supplementary Table 4: Parameters in transmission equation for HTNV.

Parameters	Estimations
$\log\beta_{rain}$	(0.01, 0.02, 0.03, 0.02, 0.01, 0.01, 0.00, 0.00, 0.00, 0.00, 0.00)
$\log\beta_{temp}$	(-0.05, -0.03, -0.02, 0.00, 0.00, 0.00, 0.01,0.03, 0.04, 0.02, 0.01)
α	-0.61
γ	-0.68

The exponents α and γ are mixing parameters. $\log\beta_{rain}$ is the effect of rainfall on virus transmission rate. $\log\beta_{temp}$ is the effect of temperature on virus transmission rate.

References

1. Dammhahn, M. *et al.* Of city and village mice: behavioural adjustments of striped field mice to urban environments. *Sci. Rep.* **10**, 13056 (2020).
2. Tulis, F. *et al.* The impact of the striped field mouse's range expansion on communities of native small mammals. *Sci. Rep.* **13**, 753 (2023).
3. Szacki, J., & Liro, A. Movements of small mammals in the heterogeneous landscape. *Landsc. Ecol.* **5**, 219-224 (1991).
4. Tulis, F. *et al.* Expansion of the Striped field mouse (Apodemus agrarius) in the south-western Slovakia during 2010–2015. *Folia Oecologica* **43**, (2016).
5. Timm, R. M. Norway rats. *The handbook: prevention and control of wildlife damage*, (1994).
6. Lambert, M. S. *et al.* The effect of habitat management on home-range size and survival of rural Norway rat populations. *J. Appl. Ecol.* **45**, 1753-1761 (2008).
7. Costa, F. *et al.* Multiple paternity in the Norway rat, Rattus norvegicus, from urban slums in Salvador, Brazil. *J. Hered.* **107**, 181-186 (2016).
8. GARDNER-SANTANA, L. C. *et al.* Commensal ecology, urban landscapes, and their influence on the genetic characteristics of city-dwelling Norway rats (Rattus norvegicus). *Mol. Ecol.* **18**, 2766-2778 (2009).
9. Tong L. *et al.* Influence of intra-and inter-specific competitions on food hoarding behaviour of buff-breasted rat (Rattus flavipectus). *Ethol. Ecol. Evol.* **24**, 62-73 (2012).
10. Vial, P. A. *et al.* Hantavirus in humans: A review of clinical aspects and management. *The Lancet Infect. Dis*. (2023).
11. Tian HY *et al.* Urbanization prolongs hantavirus epidemics in cities. *Proc. Natl. Acad. Sci. U.S.A.* **115**, 4707-4712 (2018).
12. Suzan, G. *et al.* The effect of habitat fragmentation and species diversity loss on hantavirus prevalence in Panama. *Ann. N. Y. Acad. Sci.* **1149**, 80-83 (2008).
13. Magnusson, M. *et al.* Spatial and temporal variation of hantavirus bank vole infection in managed forest landscapes. *Ecosphere*, **6**, 1-18 (2015).
14. Shilova, S. A., & Tchabovsky, A. V. Population response of rodents to control with rodenticides. *Curr. Zool.* **55**, 81-91 (2009).